JOURNAL OF GEOPHYSICAL RESEARCH, VOL. 103, NO. A1, PAGES 93–102, JANUARY 1, 1998

Identification of magnetospheric particles that travel between spacecraft and their use to help obtain magnetospheric potential distributions

E. C. Whipple, [1] J. S. Halekas, [1] J. D. Scudder, [2] W. R. Paterson, [2] L. A. Frank, [2] R. B. Sheldon, [3] N. C. Maynard, [4] D. R. Weimer, [4] C. T. Russell, [5] K. Tsuruda, [6] H. Hayakawa, [6] and T. Yamamoto [6]

Abstract. We identify magnetospheric ions from Hydra on Polar and comprehensive plasma instrument on Geotail that have traveled between these spacecraft at three times at half-hour intervals from 1800 to 1900 UT on August 19, 1996. During this time the activity level was low, the magnetosphere was quiet, and inductive electric fields should have been minimal. The identification is made by first using the magnetic fields measured by Magnetic Field Experiment (Polar) and magnetic field instrument (Geotail), together with the Tsyganenko 1996 magnetic field model to calculate the mapping of pitch angles between spacecraft. We then make a one-parameter search in energy, and equivalently in the space defined by the first two adiabatic invariants, to find matchings in the ion velocity distribution functions as predicted by Liouville's theorem. We find matchings at these three times, with each matching occurring over the appropriate ranges of pitch angles and at a unique difference in kinetic energy. We interpret the difference in kinetic energy as a measure of the potential difference between the regions of the two spacecraft. These differences are consistent with the potential changes along each spacecraft path during this time from the electric fields measured by electric field instrument (Polar) and electric field detector (Geotail) and from a map of estimated magnetospheric potential distribution for the existing activity levels. Spacecraft positions when plotted in the (U, B, K) coordinate system confirm that ion travel between the spacecraft was possible during this time period. This technique for identifying particles traveling between spacecraft should be a valuable tool for correlating spectral features seen in particle data by different spacecraft in the magnetosphere.

1. Introduction

One of the major goals of the International Solar-Terrestrial Program is to use observations from different spacecraft to gain understanding of magnetospheric processes. Yet the correlation of spectral features in particle data seen by different spacecraft is a thorny problem because of the complicated dependence of particle trajectories on energy and pitch angle and the resulting uncertainty in the quantitative identification, analysis, and interpretation of apparently similar features seen by different spacecraft.

We seek to demonstrate in this paper that it is possible to identify magnetospheric charged particles that travel between pairs of spacecraft. If this were done as a function of spacecraft positions as they move, a mapping could be provided between particle spectra obtained in different regions. Thus particle detectors could become tracer experiments and make remote sensing measurements of the magnetosphere in much the same way that charged particle beams have been used. The problem of course is to identify which particles, if any, have traveled from the vicinity of one spacecraft to that of another.

The technique that we use is based on use of the first two adiabatic invariants of charged particle motion, on

[1]Geophysics Program, University of Washington, Seattle, Washington.

[2]Department of Physics and Astronomy, University of Iowa, Iowa City, Iowa.

[3]Center for Space Physics, Boston University, Boston, Massachusetts.

[4]Mission Research Corporation, Nashua, New Hampshire.

[5]Institute of Geophysics and Planetary Physics, University of California at Los Angeles.

[6]Institute of Space and Astronautical Science, Sagamihara, Kanagawa, Japan.

Paper number 97JA02195.
0148-0227/98/97JA-02195$09.00

the use of magnetic field models of the magnetosphere, and on the use of Liouville's theorem. We compare particle data from the Polar and Geotail spacecraft during the interval 1800-1900 UT on August 19, 1996, when the magnetosphere was quiet and when therefore the magnetic field was reasonably stationary and inductive electric fields should be minimal. We use the Tsyganenko 1996 magnetic field model together with the measured magnetic field at the two spacecraft to calculate the pitch angle ranges of particles that could travel between the spacecraft. We show how the use of (U, B, K) coordinates (U, electric potential; B, magnetic field magnitude, $K(\mathbf{r}) = \oint \sqrt{B(\mathbf{r}) - B(s)}ds$) can determine whether particle access is possible between different regions [*McIlwain,* 1972; *Whipple,* 1978; *Sheldon and Gaffey,* 1993; *Sheldon,* 1994]. $K(\mathbf{r})$ is the modified longitudinal invariant which has the property that it depends only on position and not on any particle properties [*Kaufmann,* 1965; *Roederer,* 1970]. We then use two different but equivalent techniques to compare the measured distribution functions, $f(\mathbf{v})$, from each spacecraft over the appropriate range of pitch angles and energy, or equivalently of magnetic moment μ and K, and look for a match in $f(\mathbf{v})$. We find such matches as a line in (μ, K) space which has a specific, predictable shape, and from the constant energy difference between these particles at the two spacecraft we infer the value of ΔU between the two regions. (The potential U should not be confused with spacecraft potentials caused by charging.)

The electric field is an especially important quantity in the magnetosphere in that it is the energization mechanism for charged particles and is therefore an essential element for understanding magnetospheric processes. The electric field is difficult to measure [*Pedersen et al.,* 1984; *Gustafsson et al.,* 1997; *Paschmann et al.,* 1997] and is much more variable than the magnetic field, and there is therefore a scarcity of good models of the magnetospheric electric field. Potential distributions have been obtained [e.g., *McIlwain,* 1972; *Stern,* 1973; *Volland,* 1973], some of these by mapping up magnetic field lines from the ionosphere with the assumption that magnetic field lines are equipotentials [*Weimer,* 1995, 1996; *Maynard et al.,* 1995]. This is a reasonable assumption in parts of the magnetosphere during quiet times (which we use in this paper) but is not a good assumption during active times when inductive fields become important. In this paper we demonstrate that it is possible to connect measurements of the electric field made by different spacecraft by using particles traveling between the spacecraft to establish the potential difference between the regions.

Data from the following instruments were used in this study: plasma data from the Hydra instrument on Polar [*Scudder et al.,* 1995] and from the comprehensive plasma instrument (CPI) on Geotail [*Frank et al.,* 1994]; electric field data from the electric field instrument (EFI) on Polar [*Harvey et al.,* 1995] and from the electric field detector (EFD) on Geotail [*Tsuruda et al.,* 1994]; magnetic field data from the Magnetic Field Experiment (MFE) on Polar [*Russell et al.,* 1995] and from the magnetic field instrument (MGF) on Geotail [*Kokubun et al.,* 1994].

In the following section we present a detailed description of how this analysis and comparison was done at one time, 1830 UT on August 19, 1996. We then give the results for the times of 1800 and 1900 UT, and compare these potential differences inferred from the particle data with those that might be expected from the electric field measurements on the two spacecraft and from a map of magnetospheric potential distribution based on statistical studies for the existing activity levels.

2. Treatment of Particle Data at 1830 UT

2.1. Assumptions and Choice of Time

The assumptions made in this analysis are as follows: (1) The magnetospheric electric field is electrostatic and that therefore inductive electric fields are negligible. This also implies that the magnetic field is static over at least the drift times of the particles. (2) There is no electric field parallel to the magnetic field and that therefore field lines are equipotentials. (3) The charged particles that we study are collision-free with negligible sources or sinks along their trajectories between spacecraft so that Liouville's theorem is valid. (4) The *Tsyganenko* [1995] 1996 magnetic field model is reasonably accurate over this region of the magnetosphere. This assumption can be verified by comparison with the onboard measurements of B (see Table 1). The model somewhat overestimates B_z at Geotail.

We selected the time period of 1800-1900 UT, August 19, 1996, because at this time both the Geotail and Polar spacecraft passed through the near-tail region of the magnetosphere, and the activity levels of the magnetosphere were very low. The Kp levels and GSM coordinates of of the two spacecraft are shown in Table 1 for the three selected times. Although the two spacecraft were fairly distant from each other during this interval, the magnetic field lines on which the spacecraft were situated were reasonably close together (at 1830 UT they were about 3 R_E apart in the magnetic equator).

Figure 1 shows a high-latitude electric field model for the existing interplanetary conditions during this time period [*Weimer,* 1995, 1996; *Shue and Weimer,* 1994] (B_y = -1.2 nT, B_z = 2.0 nT, and V_{SW} = 400 km/s). This model is mapped from the high-latitude ionosphere into the GSM equator using the Tsyganenko 1996 magnetic field model and superimposed with the Earth's corotation potential. Also shown as symbols in Figure 1 are the GSM equatorial crossings of the magnetic field lines on which Polar and Geotail are situated at the three half-hour times of 1800, 1830, and 1900 UT. Both spacecraft are moving toward the bottom of the map

Table 1. *Kp* levels, GSM Coordinates, and Magnetic Field

Time	*Kp* Level	Polar			Geotail		
		X	Y	Z	X	Y	Z
1800	1	-1.05	-3.05	2.93	-10.86	-6.66	1.80
1830	< 1	-0.71	-3.17	3.88	-10.71	-7.46	1.74
1900	< 1	-0.35	-3.20	4.67	-10.55	-7.99	1.62

		Polar			Geotail		
Time	Source	B_x	B_y	B_z	B_x	B_y	B_z
1800	Meas.	294.33	432.77	-72.72	-8.36	-6.08	3.98
1800	Model	288.22	440.90	-88.75	-5.11	-8.49	9.22
1830	Meas.	164.40	304.46	-161.45	-6.38	-6.20	4.99
1830	Model	162.82	313.11	-170.52	-0.85	-6.91	9.59
1900	Meas.	95.18	214.54	-171.38	-2.45	-3.15	5.46
1900	Model	98.55	225.67	-178.64	0.87	-5.87	10.07

GSM coordinates are in R_E and magnetic field is in nanoteslas.

(toward dusk) during this time. The potential contours on the map have been referenced to 0 V at the Polar spacecraft location at 1830 UT. Figures 2 and 3 show the magnetic and electric field as measured by the instruments on Polar (Figure 2) and on Geotail (Figure 3) for the 1-hour time interval.

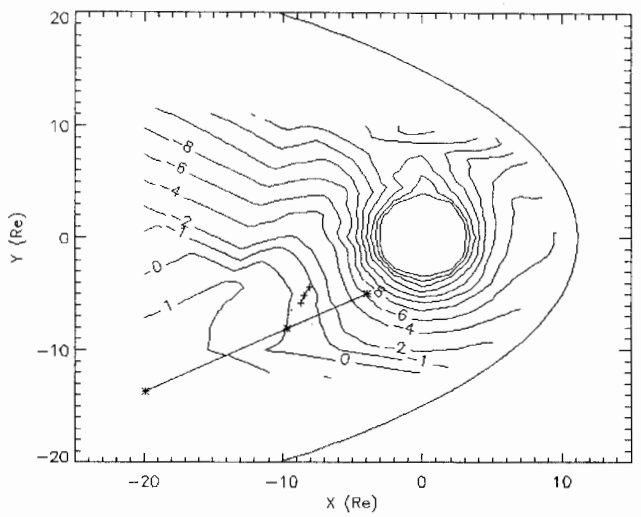

Figure 1. Map of potential distribution projected to the GSM equatorial plane for the existing activity levels during this period based on the *Weimer* [1996] model. The positions of the spacecraft field lines are shown at the three times (asterisk, Polar; plus, Geotail, both spacecraft are moving toward the lower left). The level for the potential map has been chosen to be zero at the Polar field line location at 1830 UT. The contour levels are shown in kilovolts. The magnetopause is taken from the Tsyganenko 1996 model.

2.2. Magnetic Field Line Calculations

The mapping procedure for finding the particles that travel between spacecraft is illustrated schematically in Figure 4. We used the Tsyganenko 1996 model to calculate the magnetic field and the value of the invariant K along each of the two field lines through each spacecraft, shown as $B_P(K)$ and $B_G(K)$ in Figure 5. Particles at one spacecraft, say Geotail, with a measured pitch angle (α_{Gi}) travel up the field line until their pitch angle reaches 90 °; the value of K at which this occurs (call this K_i) is determined from the constancy of the magnetic moment and therefore by the values of the magnetic field at Geotail, B_{Geo} , and at the mirror point, $B_G(K_i)$:

$$B_G(K_i) = \frac{B_{Geo}}{\sin^2 \alpha_{Gi}} \tag{1}$$

The particle mirror point can then be considered to drift on this constant K_i surface. If K_i is greater than or equal to that at the Polar spacecraft, i.e., $K_i > 800\sqrt{\text{nT}}R_E$, and if the particle has the right energy (to be found later) it will intercept the Polar field line where that field line goes through the same K_i surface. Thus we know from the $B_P(K)$ curve what the magnetic field is at that point, and therefore can calculate the pitch angle when the particle bounce motion takes it down the magnetic field line to the Polar spacecraft from a relation similar to (1):

$$\sin^2 \alpha_{Pi} = \frac{B_{Pol}}{B_P(K_i)} \tag{2}$$

We restrict our use of K to values allowed for particles to travel between the spacecraft, i.e., to values of K

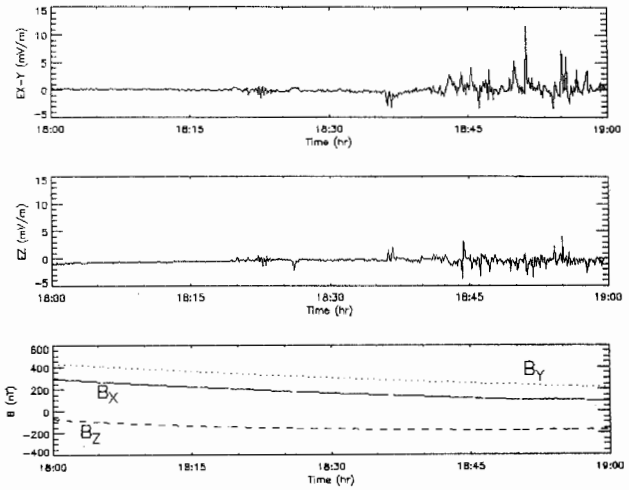

Figure 2. Electric and magnetic field measurements on Polar for 1800-1900 UT, August 19, 1996. *EX-Y* and *EZ* are de-spun values in the spacecraft spin plane. The spin axis component is not shown because it is more susceptible to error than the other two components. The spin axis component did not contribute to the potential along the Polar path (shown in Figure 11) since the Polar orbit was perpendicular to its spin axis. Unit vectors in the *X-Y* and *Z* directions have the following GSE components respectively: (-0.606, -0.575, -0.549) and (0.0, -0.691, 0.723). The components of *B* are in the GSM coordinate system.

greater than that at the Polar spacecraft ($800\sqrt{\mathrm{nT}}R_E$), and less than $2000\sqrt{\mathrm{nT}}R_E$, which corresponds to an altitude of about 2 R_E in the polar regions. The latter constraint was chosen so that we would not deal with particles mirroring in the interaction region too close to the Earth's ionosphere. From these calculations we arrive at a range of pitch angles at each spacecraft, with a one-to-one correspondence between them (labeled by K), which identify those pitch angles at each spacecraft that particles must have in order to travel between the two spacecraft at this time. Note that this calculation does not depend on the particle species, energy, nor on the direction of travel. These remain to be found.

2.3. The (U, B) Plot in the K Surface Going Through Polar

Figure 6 is a plot using (U, B) coordinates in the constant K surface corresponding to the value of K (call this K_{Pol}) at Polar ($K_{Pol} = 800\sqrt{\mathrm{nT}}R_E$). The values of B for the two spacecraft field lines where they intersect this surface are known from the model magnetic field as shown in Figure 5. We have located the two spacecraft field lines in this surface using these values of B and values of the potential U which we determined from the $f(\mathbf{v})$ comparison described below. We have shown before that particle mirror points travel in a straight line in this kind of plot. The drift motion is a combination of the electric field drift and the magnetic gradient and curvature drifts and is determined by (total) energy conservation and thus is automatically averaged over the particle bounce motion [*Whipple*, 1978]. The slope of this line is known from energy conservation:

$$slope = (-\mu/e) = \frac{\Delta U}{\Delta B} \tag{3}$$

where e is the particle charge, $\Delta U = U_G - U_P$, and $\Delta B = B_G(K) - B_P(K)$. Thus ions have a negative slope and electrons a positive slope. The consistency of the slope from this relation is used later as a test of the results. We also know from the constancy of the magnetic moment and from the conservation of total energy that the kinetic energies E of a particle on the two field lines are related by

$$\begin{aligned} E_G/E_P &= B_G(K)/B_P(K) \\ E_G - E_P &= -e\Delta U \end{aligned} \tag{4}$$

Thus we have two relations involving the two energies and the value of ΔU, but all three of these are at the moment still unknown. We invoke Liouville's theorem to provide the final relation that is needed to identify ΔU, namely that the distribution functions should be identical for particles that are seen at both spacecraft. Each value of K provides a different $\Delta B(K)$ and ratio $B_G(K)/B_P(K)$, but if the assumptions, reasoning, and measurements are valid, then each comparison (as a function of K) should give the same ΔU.

We note from Figure 5 that at 1830 UT the values of $B_G(K)$ are consistently higher than $B_P(K)$. This means that the particles have higher energy at Geotail than at Polar and therefore the potential at Geotail is lower (higher) at Geotail than at Polar if the species are

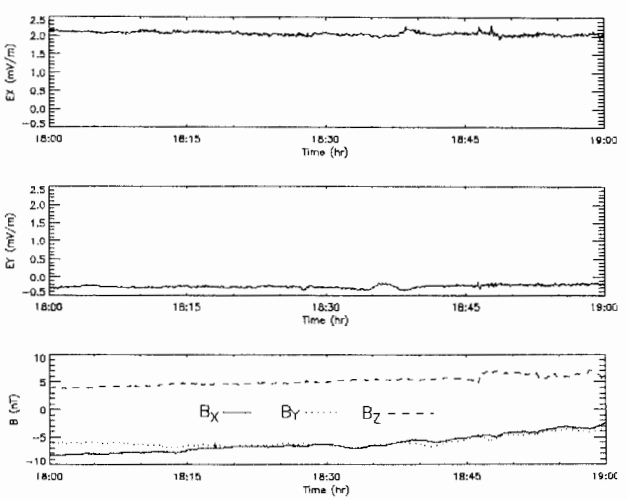

Figure 3. Electric and magnetic field measurements on Geotail for 1800-1900 UT, August 19, 1996. *EX* and *EY* are de-spun values in the spacecraft spin plane and are close to the GSE X and Y directions. *EX* has an undetermined offset, and only the variations should be considered significant. Only *EY* was used to obtain the potential change along the spacecraft path. The components of B are in the GSM coordinate system.

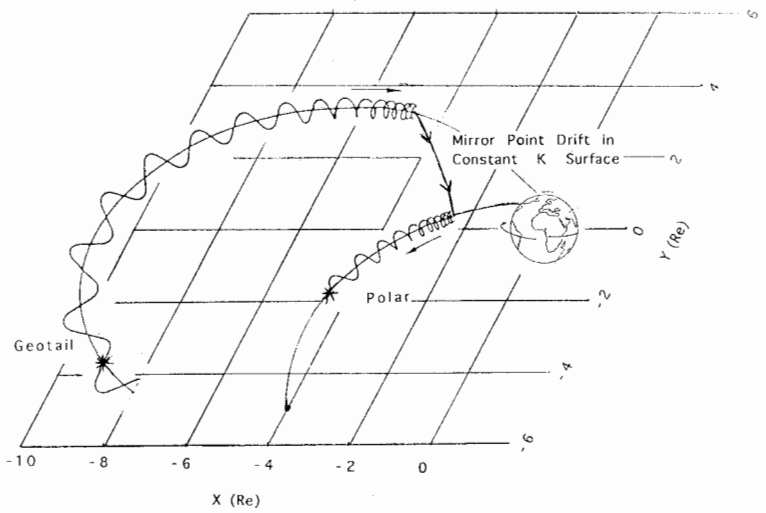

Figure 4. Schematic illustration of the travel of particles between Geotail and Polar at 1800 UT. The magnetic field line going through each spacecraft is shown above the GSM equator (the gridded plane). Geotail is above the GSM equator but slightly below the $K = 0$ surface.

ions (electrons). The direction of motion is determined by the value of the generalized velocity function W and the equations of motion [*Whipple*, 1978]:

$$\begin{aligned} dB/dt &= W \\ dU/dt &= -(\mu/e)W \\ dK/dt &= 0 \end{aligned} \tag{5}$$

$$W = \frac{(\nabla U X \nabla B) \cdot \nabla K}{\vec{B} \cdot \nabla K} \tag{6}$$

The W = 0 curves for the K_{Pol} surface are also shown in Figure 6. These curves represents the dividing line between the tail (where particles gain kinetic energy) and the front (where particles lose kinetic energy), but it is possible to use the one plot for both tail and front with the understanding that particles travel towards higher B in the tail but towards lower B in the front.

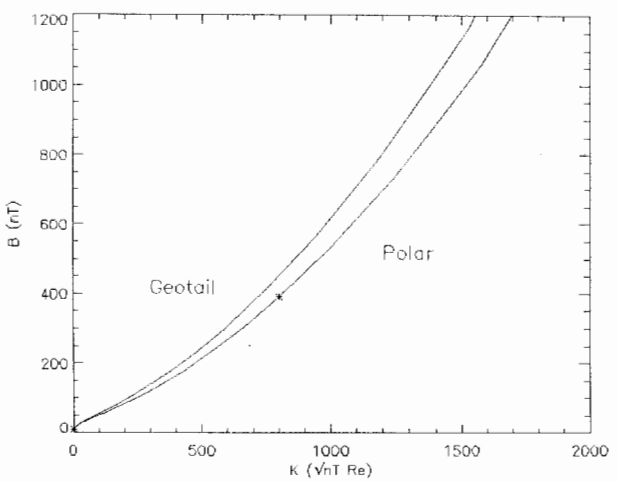

Figure 5. Magnetic field versus the invariant K for the two magnetic field lines going through Polar and Geotail at 1830 UT. The locations of the two spacecraft are indicated by asterisks.

By using the model magnetic field and the map of estimated potential distribution (Figure 1) we find that W is positive at Geotail and at Polar at all three times, although irregularities in the map of potentials made the calculation difficult. From the relative positions of Geotail and Polar in this plot we infer that ions have traveled from the vicinity of Polar toward the higher B and lower U at Geotail at 1830 UT, but from Geotail to Polar at 1800 UT. We show the position of the Polar field line in this plot at 1900 UT, but travel between the spacecraft by drifting on this K surface of 800 $\sqrt{\text{nT}}R_E$ is not possible at this time since $B_P(K{=}800)$ at 1900 UT is less than at the Polar spacecraft (but travel is possible at higher K values). The value for W at Polar from the potential map was ~5 nT/s. From this an estimate of the drift time for the ions to travel from Polar to Geotail can be made from (5): namely, $\Delta t = \Delta B(K)/W \approx$(20 nT)/(5 nT/s) $\approx$ 4 s.

3. Comparisons of Distribution Functions

We have used two methods to search for a match between distribution functions from the two spacecraft using Polar Hydra data and Geotail CPI data. The first method works with the allowed energies and pitch angles at each spacecraft. We first assume a value for ΔU; this enables us to calculate the energies at the two spacecraft at which the match might occur as a function of K, from the two equations in (4). These are shown in Figure 7, for the ΔU at which the match was found, as a function of the parameter K at the time 1830 UT. These values of K give the appropriate pitch angles at the spacecraft from (1) and (2), which are also shown in Figure 7.

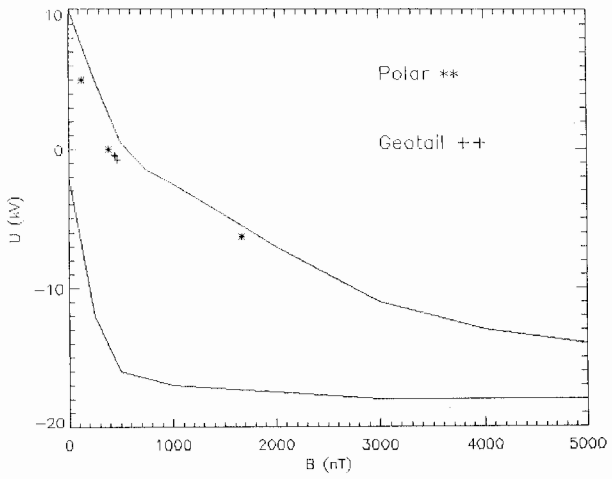

Figure 6. Plot of the $W = 0$ curves in (U, B) coordinates in the constant K surface that intersects Polar at 1830 UT. The positions of the Polar and Geotail magnetic field lines are also shown at 1800, 1830, and 1900 UT (both spacecraft are moving toward lower B; the last two positions of Geotail overlap). The $W = 0$ curves are boundaries between the tail ($W > 0$) and the front ($W < 0$) of the magnetosphere. Mirror points follow straight lines toward higher B in the tail and towards lower B in the front; ions have a negative and electrons a positive slope.

In these comparisons we were working at times with quite low count rates in the ion measurements. We therefore fitted the velocity distribution functions at each energy to a linear expression in pitch angle to remove some of the fluctuations in the values of $f(\mathbf{v})$ caused by the low number of counts. We also folded over the values of $f(\mathbf{v})$ from pitch angles greater than 90° to their complement below 90° (which give the same K) in carrying out the fitting procedure. We then interpolated in energy between these fitted curves to find $f(\mathbf{v})$ for the appropriate (E, α) or (μ, K) required for the comparisons. Figure 8 shows the Polar data points from Hydra (for every third energy) that were used at 1830 UT and the corresponding fitted curves.

We form the sum of the squares of the difference in the normalized distribution functions taken from the fitted curves over this range of E and α to calculate a chi-squared summation:

$$\chi^2 = \sum_i [f_G(\mathbf{v}_{Geo}, i) - f_P(\mathbf{v}_{Pol}, i)]^2 / {\sigma_{f,i}}^2 \qquad (7)$$

and calculate this sum systematically for a range of values for ΔU. The index i refers to the set of distribution functions for the set of equally spaced values of K from that at Polar up to $K = 2000\sqrt{\text{nT}}R_E$. Each index is associated with

a particular pair of pitch angles (through K) and also with a particular pair of energies (through the mirror point magnetic fields and the value of ΔU). The denominator in (7) is the joint standard deviation for the two measurements of the particle distribution functions based on the square root of the number of counts and the calibrations of each instrument:

$$\sigma_{f,i} = \sqrt{\sigma^2_{f,i}(\text{Polar}) + \sigma^2_{f,i}(\text{Geotail})} \qquad (8)$$

We find that there is a clear minimum at some value of ΔU, and we take this value as the potential difference between the two spacecraft regions. These results for the three times are shown in Figure 9. Each summation, at a given value of ΔU, involved 15 terms. At all three times, the values of χ^2 at the minimum was of the order of or less than 15, indicating that the agreement between the two spacecraft distribution functions was significant for that value of ΔU. The values for ΔU at the three times are 3.1, -1.5, and -7.0 kV.

The other method converts the energy and pitch angle parameters for the particle instruments at each spacecraft into the corresponding values for the magnetic moment μ and longitudinal invariant K. This method makes use of the fact that since both μ and K are invariants of the particle motion, the velocity distribution functions at the two spacecraft if plotted as a function of (μ, K) should be the same for those particles seen at both spacecraft. We form a contour plot of the logarithm of the ratio of the two distribution functions, in the (μ,K) plane, shown in Figures 10a, 10b, and 10c. We find that there is a curve in this contour plot where the values approach nearest to zero, and we take that curve in (μ,K) space as an identification of those particles seen at both spacecraft. The values of μ and K along this curve identify the energies at the two spacecraft and thus the corresponding ΔU. For example, in Figure 10b there is a curve in the upper part of the figure stretching from a μ of about 12 keV/nT at $K = 800\ \sqrt{\text{nT}}R_E$ to a μ of about 8 keV/nT at $K = 2000\ \sqrt{\text{nT}}R_E$ where the values in the contour plot approach zero. Superimposed in this part of the plot are a set of asterisks. These are the values of μ as a function of K

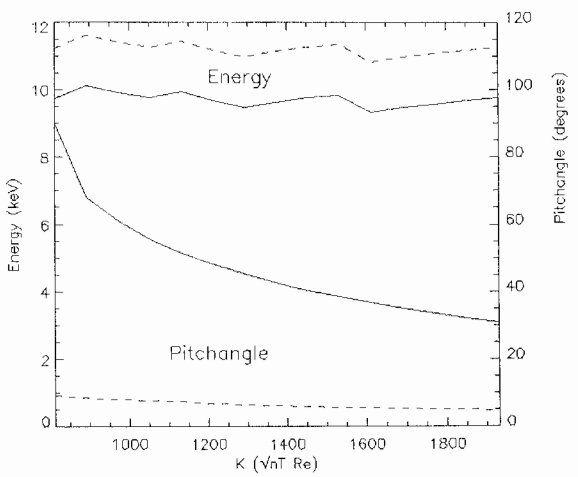

Figure 7. Allowed energies and pitch angles at each spacecraft at 1830 UT. The dashed curves are for Geotail and the solid for Polar.

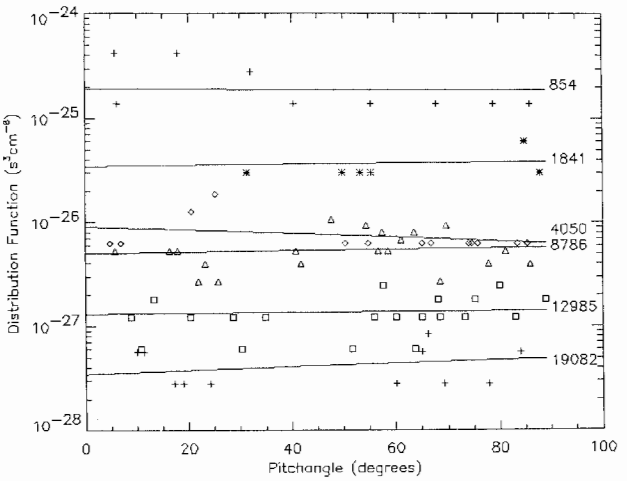

Figure 8. Polar $f(\mathbf{v})$ versus pitch angles showing data and fitted curves for every third energy channel (in eV), from the even-numbered detectors at 1830. Error bars from the count statistics are not shown to avoid clutter but can be estimated from the fact that the lowest value for f corresponds to one count.

given by the slope of the drift trajectory in the (U, B) plane for each corresponding K surface (from equation (3)):

$$\mu(K) = -e\Delta U/[\Delta B(K)] \qquad (9)$$

with the value of -1.5 kV for ΔU. It can be seen that these crosses lie on or very close to the contour closest to zero. Thus this contour is consistent with the slopes of the drift trajectories for ions drifting on different K surfaces but with a constant ΔU of -1.5 keV between the two field lines. The contour plots for the other times also show the values for $\mu(K)$ from (9) with the corresponding ΔU from Figure 9. Note that the comparison in Figure 9 gives a global test on the agreement of distribution functions (i.e., a sum over the points in velocity space) whereas the comparisons in Figure 10 give a point by point test along the line in (μ, K) space.

4. Comparison with Electric Field Measurements and Model

We have integrated the electric field as measured by EFI on Polar and by EFD on Geotail along each spacecraft path during the time interval from 1800 to 1900 UT. These potentials plotted as a function of time are shown in Figure 11 as solid curves. We have arbitrarily set the potential at Polar at 1830 UT to be 0 V, and have placed the potential curve measured along the Geotail path so that it goes through the potential of -1.5 kV at 1830, as indicated by the vertical arrow at that time. This is the inferred difference derived above for the (Geotail - Polar) potential difference. Thus we use the potential difference obtained from the particle data to interconnect electric field measurements obtained on different spacecraft. We envisage this as one of the important applications of our technique for identifying particles that travel between spacecraft.

We also show by vertical arrows in Figure 11 the potential differences (magnitude and direction) obtained from the particle data at the times 1800 and 1900 UT. These differences are consistent with the measurements of potential change along the spacecraft paths as measured by the onboard electric field instruments, although the difference between the potentials derived from the onboard electric field measurements indicate a somewhat greater change in the potential differences over the hour's time between the two regions than is obtained from the particle measurements. We note that the electric field magnitude measured on Geotail in the GSE Y direction during this time was very small, of the order of 0.25 mV/m. Since this is near the sensitivity of the measurement, it is possible that the potential change calculated along the Geotail path is an upper limit. The electric field measured on Polar was typically of the order of 2 mV/m (the spin axis component is not known well).

The dashed curves in Figure 11 are the model potentials as read from the map of Figure 1 for the spacecraft magnetic field lines during this time interval. Again, there is reasonable consistency between the dashed curves and the potential differences (vertical arrows) between Polar and Geotail determined by the particles at the three times.

5. Comments and Conclusion

We have not tried yet to make error estimates in our identification of such particles or in the potential differences that we have inferred. There are obviously a number of possible difficulties and sources of error in our procedure. We list some of these here without trying to evaluate them quantitatively.

In the comparison of particle distribution functions we are dependent on accurate calibrations of the particle instruments on the two spacecraft. The particle

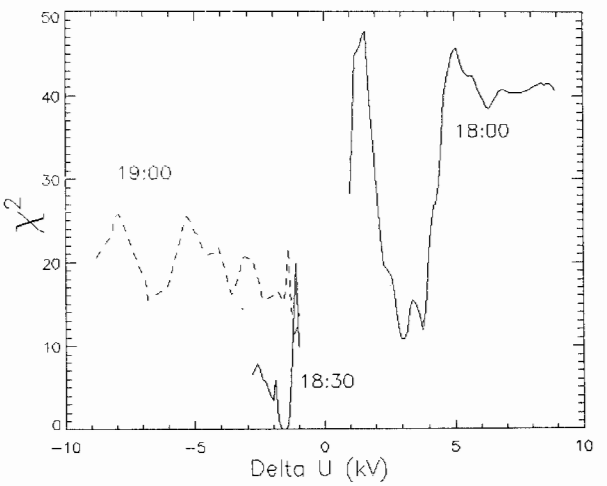

Figure 9. Plot of $\chi^2 = \sum [f_G(\mathbf{v}) - f_P(\mathbf{v})]^2/{\sigma_f}^2$ versus ΔU for the three times. The steps in ΔU were 0.1 keV.

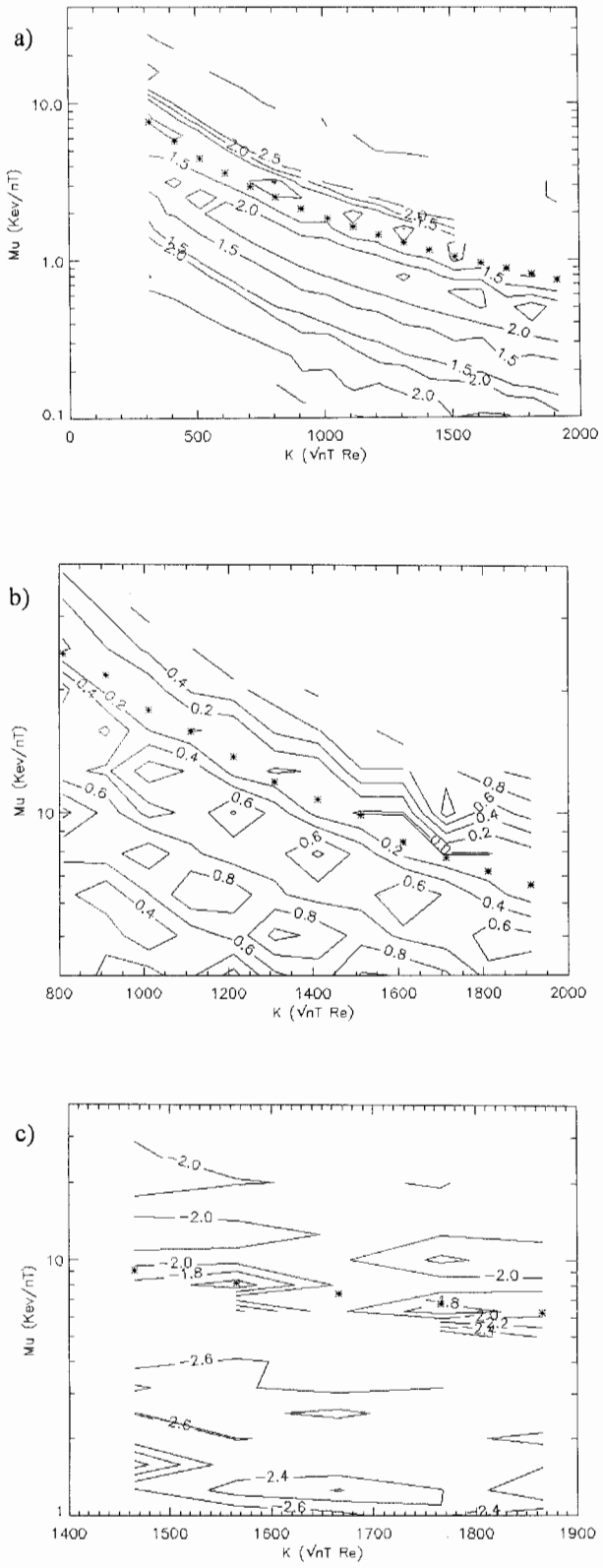

Figure 10. Contour plots of $\ln[f_G(\mathbf{v})/f_P(\mathbf{v})]$ in the (μ, K) plane: (a) at 1800, (b) at 1830, and (c) at 1900. The contour nearest to zero is taken as the identification of ions travelling between the spacecraft. The asterisks are $\mu(K)$ from (9), where the value of ΔU is the same as found from Figure 9 for the three times.

pitch angle binning relies on the accuracy of the magnetic field measurements on the two spacecraft, and the mapping of pitch angles between the spacecraft relies on the Tsyganenko 1996 magnetic field model and on the choice of activity parameters that go into that model. The comparison of potential differences with the electric field measurements are dependent on the calibration of the electric field instruments. Probably the largest uncertainty in our work comes from the process of integrating along the model magnetic field lines to obtain $B(K)$. However, this affects mainly the pitch angle relation between the two spacecraft, and for fairly isotropic velocity distributions such as we have been working with in this study, the uncertainties due to errors in pitch angle determination may not be large. However, it is true that the difference and ratio of magnetic fields at the particle mirror points enter into the determination of the appropiate energies of the particles, and into the test of the drift relations involved in matching $f(\mathbf{v})$. We do not know what errors might have been introduced by any of these considerations.

We have noticed that in some of the comparisons of $f(\mathbf{v})$ (not discussed elsewhere) that there can be "accidental" agreements between the distribution functions in different parts of velocity space (typically at low energies of a few hundred eV) than where we have identified the particles as common to both spacecraft. Our determination was partly based on the consistency of the progression of the potential differences with the on-

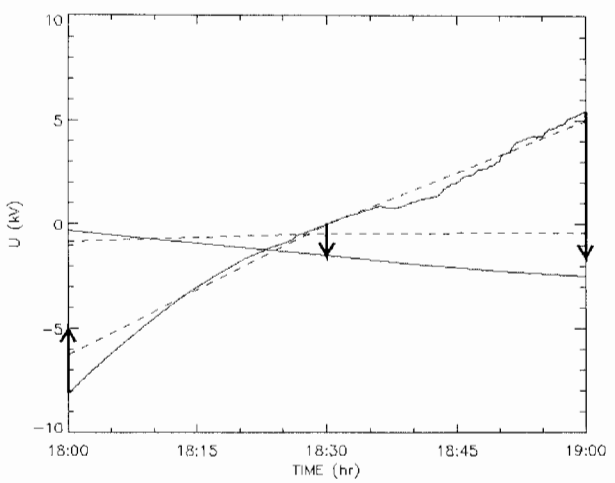

Figure 11. Potentials along the spacecraft paths from 1800 to 1900 UT from the onboard electric field measurements (solid curves) and also from the map of potential distribution (dashed curves) based on the *Weimer* [1996] model. The two Polar curves are forced to go through zero potential at 1830 UT and the Geotail solid curve through -1.5 kV at 1830 UT. (The Polar electric field measurements are questionable before 1815 UT.) The vertical arrows at the three times indicate the values of the potential differences ΔU found from the particle data: 3.1 kV, -1.5 kV, and -7.0 keV.

board electric field measurements and with what in general is expected for the magnetospheric electric field, as demonstrated by the potential map based on existing conditions. Such accidental agreements are probably to be expected at times, especially when the $f(\mathbf{v})$ are nearly isotropic since matching $f(\mathbf{v})$ in such a case depends mainly on the energy variation. We note that having a larger variation in both $B_G(K)/B_P(K)$ and $B(K)$ as a function of K would provide a clearer identification of matching because of a larger variation in energy ratios and differences over the allowed range of K.

It can be seen from (3) that the kinetic energy of particles at which matching $f(\mathbf{v})$ can be found for a given ΔU can be estimated to be of the order of $|e\Delta U B(K)/\Delta B(K)|$. Thus for moderate or large $|\Delta U|$ but small $|\Delta B|$ one can expect to find matchings to occur at high energies. This relation can help to guide in the choice of particle data in the search for matchings.

We have neglected possible gyrophase dependence of the particle distribution functions, and we note in this connection that particles at the same energy but with different gyrophases at a spacecraft will be drifting on slightly different paths because it is the particle energy at the gyrocenter that determines drift across equipotentials. At the Polar ion energy of 10 keV where there was ion matching at 1830 UT (Figure 7), the gyroradius for protons is of the order of 37 km. For the measured electric fields at Polar of about 2 mV/m, the potential change across a gyrodiameter would be about 150 V. This would introduce some smearing in energy of the $f(\mathbf{v})$ comparisons with consequent uncertainties in the inferred potential differences.

It is striking that in spite of all the possible sources of error, the inferred potential differences between the two spacecraft regions are as consistent as shown with other estimates of those potential differences (Figure 11). These results demonstrate that it is possible to identify charged particles which have traveled between two spacecraft and that useful information about the magnetosphere can be extracted from the properties of these particles. In addition to the inference of potential differences and the mapping of particle spectra between different spacecraft measurements mentioned in the introduction, a number of other possible applications of this new tool can be imagined. We leave the consideration of these for future work.

Acknowledgments. We thank G. Parks for his encouragement and support of this work through NASA Space grant NGT5-40017 at the University of Washington. We thank S. Kokubun for permission to use data from the magnetic field instrument (MGF) on Geotail and F. Mozer for his advice and permission to use data from the electric field instrument (EFI) on Polar. The results of this paper were made possible by Hydra NASA funding under grant NAG 5-2231 to the University of Iowa, and DARA grant 50-OC 8911-0. The present results of the Hydra investigation would not have been possible without the decade-long hardware efforts led by groups at NASA GSFC by K. Ogilvie, at UNH by R. Torbert, at Max Planck Institute Lindau by A. Korth, and at UCSD by W. Fillius. The work at Boston University was supported by NASA grant NAS5-97147, at the University of California at Los Angeles by NASA grant NAG5-3171, and at Mission Research Corporation by NASA through the University of California at Berkeley under grants NAS 5-30367 and NAG 5-3182.

The Editor thanks T. E. Eastman and another referee for their assistance in evaluating this paper.

References

Frank, L. A., K. L. Ackerson, W. R. Paterson, J. A. Lee, M. R. English, and G. L. Pickett, The comprehensive plasma instrumentation (CPI) for the Geotail spacecraft, *J. Geomagn. Geoelectr., 46,* 23-37, 1994.

Gustafsson, G., et al., The electric field and wave experiment for the Cluster mission, *Space Sci. Rev.,79,* 137-156, 1997.

Harvey, P., et al., The electric field instrument on the Polar satellite, *Space Sci. Rev., 71,* 583-596, 1995.

Kaufmann, R. L., Conservation of the first and second adiabatic invariants, *J. Geophys. Res., 70,* 2181-2186, 1965.

Kokubun, S., T. Yammamoto, M. H. Acuna, K. Hayashi, K. Shiokawa, and H. Kawano, The Geotail magnetic field experiment, *J. Geomagn. Geoelectr., 46,* 7-22, 1994.

Maynard, N. C., W. F. Denig, and W. J. Burke, Mapping ionospheric convection patterns to the magnetosphere, *J. Geophys. Res., 100,* 1713-1721, 1995.

McIlwain, C. E., Plasma convection in the vicinity of the geosynchronous orbit, in *Earth's Magnetospheric Processes,* edited by B. M. McCormac, pp. 268-279, D. Reidel, Norwell, Mass., 1972.

Paschmann, G., et al., The electron drift instrument for Cluster, *Space Sci. Rev., 79,* 233-269, 1997.

Pedersen, A., C. Cattell, C.-G. Falthammar, V. Formisano, P.-A. Lindqvist, F. S. Mozer, and R. B. Torbert, Quasistatic electric field measurements with spherical double probes on the GEOS and ISEE satellites, *Space Sci. Rev., 37,* 269-312, 1984.

Roederer, J. G., *Dynamics of Geomagnetically Trapped Radiation,* Springer, New York, 1970.

Russell, C. T., R. C. Snare, J. D. Means, D. Pierce, D. Dearborn, M. Larson, G. Barr, and G. Le, The GGS/Polar magnetic fields investigation, *Space Sci. Rev., 71,* 563-582, 1995.

Scudder, J., et al., Hydra–A 3-dimensional electron and ion hot plasma instrument for the Polar spacecraft of the GGS mission, *Space Sci. Rev., 71,* 459-495, 1995.

Sheldon, R. B., Plasma sheet convection into the inner magnetosphere during quiet conditions, in *Solar Terrrestrial Energy Program: COSPAR Colloquia Series.* vol. 5, edited by D. N. Baker, pp. 313-318, Pergamon, Tarrytown, N. Y., 1994.

Sheldon, R. B., and J. D. Gaffey, Particle tracing in the magnetosphere: New algorithms and results, *Geophys. Res. Lett., 20,* 767-770, 1993.

Shue, J.-H., and D. R. Weimer, The relationship between ionospheric convection and magnetic activity, *J. Geophys. Res., 99,* 401-415, 1994.

Stern, D. P., A study of the electric field in an open magnetospheric model, *J. Geophys. Res., 78,* 7292-7305, 1973.

Tsuruda, K., H. Hayakawa, M. Nakamura, T. Okada, A. Matsuoka, F. S. Mozer, and R. Schmidt, Electric field measurements on the Geotail satellite, *J. Geomagn. Geoelectr., 46,* 693-711, 1994.

Tsyganenko, N. A., Modeling the Earth's magnetospheric magnetic field confined within a realistic magnetopause, *J. Geophys. Res., 100,* 5599-5612, 1995.

Volland, H., A semiempirical model of large-scale magnetospheric electric fields, *J. Geophys. Res., 78,* 171-180, 1973.

Weimer, D. R., Models of high-latitude electric potentials derived with a least error fit of spherical harmonic coefficients, *J. Geophys. Res., 100,* 19595-19607, 1995.

Weimer, D. R., A flexible IMF dependent model of high-latitude electric potentials having "space weather" applications, *Geophys. Res. Lett., 23,* 2549-2552, 1996.

Whipple, E. C., Jr., (*U, B, K*) coordinates: A natural system for studying magnetospheric convection, *J. Geophys. Res., 83,* 4318-4326, 1978.

L.A. Frank, W.R. Paterson, and J.D. Scudder, Department of Physics, University of Iowa, Iowa City, IA 52242.

J.S. Halekas and E.C. Whipple, Geophysics Program, University of Washington, P. O. Box 351650, Seattle, WA 98195. (e-mail: whipple@geophys.washington.edu)

H. Hayakawa, K. Tsuruda, and T. Yamamoto, Institute of Space and Astronautical Science, Sagamihara, Kanagawa 229 Japan.

N.C. Maynard and D.R. Weimer, Mission Research Corporation, Nashau, NH 03062.

C.T. Russell, University of California at Los Angeles, CA 90024.

R.B. Sheldon, Department of Astronomy, Boston University, Boston, MA 02215.

(Received June 12, 1997; accepted July 24, 1997.)